Virtual Correction of Eyesight using Visual Illusions

Midori Aoki, Fumihiko Sakaue and Jun Sato
Department of Computer Science and Engineering, Nagoya Institute of Technology,
Gokiso, Showa, Nagoya 466-8555, Japan

Keywords: Eyesight Correction, Visual Illusion, Lateral Inhibition, High Resolution, Deconvolution.

Abstract: Degradation of eyesight is a serious problem, and the number of weak-sighted people is increasing rapidly in recent years because of the spread of tablets and smart phones. The weak-sighted people often wear glasses and contact lenses for recovering their eyesight. However, these rectification devises are painful for weak-sighted people. Thus, in this paper, we propose a novel method for displaying visual information for weak-sighted people to see rectified images on displays. In particular, we show that visual illusions in human vision system can be used efficiently for correcting the eyesight. By using our method, weak-sighted people can see clear images on the display without wearing glasses and contact lenses. The efficiency of the proposed method is tested by using synthetic signals and real images.

1 INTRODUCTION

In recent years, many people suffer from eyesight problems. Young people often have nearsightedness because of reading textbooks, tablets etc., and old people have farsightedness because of aging. Once we have eyesight problems, we usually wear eye glasses or contact lenses. However, these glasses and contact lenses are painful, and they also cause stress to weak-sighted people.

Thus, we in this paper propose a method for correcting the eyesight of weak-sighted people virtually by showing modified images on displays. The nearsightedness and farsightedness cause depth blurs on the retina, and these depth blurs can be described by the convolution of a point spread function (PSF) with the original image.

For correcting the weak-sightedness, Alonso and Barreto (Alonso and Barreto, 2003) proposed a method for displaying deconvolution images with the PSF of weak-sightedness. However, the dynamic range of the deconvolution images becomes much larger than that of the standard displays, and thus we need to reduce the contrast of the deconvolution images, or cut out the over range signals which causes errors in eyesight correction. For showing clear images without reducing image contrast, Huang et al. (Huang et al., 2012; Wetzstein et al., 2012; Huang et al., 2014) proposed eyesight correction based on light field displays. The light field displays can control the light field emitted from the display system, and thus they enable us to concentrate lights on the retina in the eyeball, even if the eyeball has weak-sightedness. Although the light field displays can correct weak-sightedness, they require micro lens arrays in front of the display or multi-layer structure of display planes. Thus their structures are very complex, and precise calibrations of optical system are required. The light field displays also require very high resolution 2D displaying systems in general, since they control 4D light fields.

In this paper, we propose a method for showing clear images to weak-sighted people using standard displays. For this objective, we consider visual illusions in human visual systems. It is known that the human visual system observes various types of illusion, such as shape distortion, color distortion and intensity distortion. In this paper, we in particular consider visual illusion on perceived intensity. It is known that the intensity illusion occurs based on the so called *lateral inhibition* (Ratliff, 1965) in visual neurons. The lateral inhibition can be considered as a natural signal filter equipped in the human visual systems. We in this paper use the lateral inhibition of human visual systems to visualize clear images to weak-sighted people.

Aoki, M., Sakaue, F. and Sato, J.
Virtual Correction of Eyesight using Visual Illusions.
DOI: 10.5220/0005719801250130
In *Proceedings of the 11th Joint Conference on Computer Vision, Imaging and Computer Graphics Theory and Applications (VISIGRAPP 2016) - Volume 3: VISAPP*, pages 127-132
ISBN: 978-989-758-175-5

Figure 1: Chevreul illusion caused by the lateral inhibition. These five intensities are constant in each area. However, at the boundary of two different intensities, the bright intensity is observed more brightly, and the dark intensity is observed more darkly. As a result, we perceive the change in intensity in a constant intensity area.

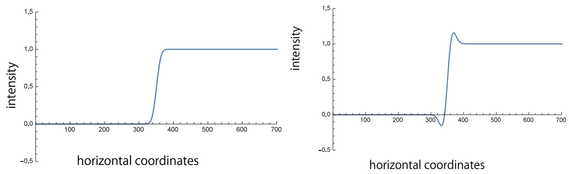

(a) original signal (b) observed signal

Figure 2: Visual illusion caused by the lateral inhibition. (a) shows the original input image signal, and (b) shows the observed signal with the lateral inhibition.

2 VISUAL ILLUSION AND LATERAL INHIBITION

We first consider visual illusion on perceived intensity. There are many types of intensity illusions, but it is known that most of the intensity illusions are based on a simple property of human visual systems, that is *lateral inhibition*. The lateral inhibition is an activity in human visual systems, in which an excited neuron suppresses the excitement of neighboring neurons in visual systems. Because of the lateral inhibition, a small difference in the input signal is emphasized in the output signal. As a result, we perceive the overshoot and undershoot of intensity at the discontinuity of original image intensity. These overshoot and undershoot in perceived intensity cause various visual illusions, such as Mach band illusion (Ratliff, 1965) and Chevreul illusion (Chevreul, 1890). Fig. 1 shows the example of Chevreul illusion, in which we perceive the change in intensity in a constant intensity area, which is caused by the overshoot and undershoot of perceived intensity at the boundary of two different intensities.

The lateral inhibition can be modeled by the difference of Gaussian (DOG) or the Laplacian of Gaussian (LOG) (Marr and Hildreth, 1980). In this paper we model the lateral inhibition by using the Laplacian of Gaussian $\nabla^2 G(x,y)$ as follows:

$$\nabla^2 G(x,y) = \frac{d^2}{dx^2}G(x,y) + \frac{d^2}{dy^2}G(x,y) \quad (1)$$

Since the output signal $S_o(x,y)$ is the sum of the original input signal $S_i(x,y)$ with the lateral inhibition, it can be described by the following convolution:

$$S_o(x,y) = L(x,y) * S_i(x,y) \quad (2)$$

where, $L(x,y)$ is a function which causes lateral inhibition, and can be described by using the Laplacian of Gaussian and the Dirac delta function $\delta(x,y)$ as follows:

$$L(x,y) = \delta(x,y) - \alpha\nabla^2 G(x,y) \quad (3)$$

α denotes the magnitude of lateral inhibition in human visual systems, and its value must be chosen empirically.

Fig. 2 shows the distortion of perceived intensity caused by the lateral inhibition modeled by Eq. (2). Fig. 2 (a) shows the original input signal and (b) shows the output signal derived from Eq. (2). As shown in this figure, the difference of intensity in the original signal has been emphasized in the output signal. The important point is that the human visual system can perceive higher intensity than the maximum intensity of display system, and can also perceive negative intensity, i.e. intensity lower than the zero level of display system. This means the human visual system can perceive wider dynamic range images than those shown on the display. In the following part of this paper, we use this property of human visual systems for correcting weak-sight in human vision efficiently.

3 PRE-FILTERING FOR WEAK-SIGHTED PEOPLE

If we have nearsightedness or farsightedness, the observed images have depth blur. This depth blur can be described by the convolution of the original input image $S_i(x,y)$ with a point spread function $P(x,y)$ as follows:

$$S_o(x,y) = P(x,y) * S_i(x,y) \quad (4)$$

Thus, if we know the point spread function $P(x,y)$ of a weak-sighted person, the clear non-blurring image can be observed by the weak-sighted person by showing the deconvolution image generated by the following equation:

$$S_i'(x,y) = P(x,y)^{-1} * S_i(x,y) \quad (5)$$

By substituting S_i' in Eq. (5) into S_i in Eq. (4), we find that the observed image $S_o(x,y)$ will be identical with the original image $S_i(x,y)$ as follows:

$$\begin{aligned} S_o(x,y) &= P(x,y) * S_i'(x,y) \\ &= P(x,y) * P(x,y)^{-1} S_i(x,y) \\ &= S_i(x,y) \end{aligned} \tag{6}$$

This method is proposed by Alonso and Barreto (Alonso and Barreto, 2003).

However, the intensity of the new input image S_i' derived from the deconvolution overflows the range of display in general, and its intensity sometimes becomes higher than the maximum intensity of the display, and sometimes becomes minus. Since the minus intensity and out of range intensity cannot be shown by the display, we have to modify the dynamic range of the deconvolution image S_i', so that its range is within the dynamic range of the display. However, this modification drastically degrades the dynamic range of the observed image. For avoiding this problem, Huand et al. (Huang et al., 2012) proposed a multi-layer display system, which consists of multiple display planes. Although is can control the light field and correcting weak-sightedness avoiding the dynamic range problem, the device structure of the multi-layer display is quite complex, and it is very difficult of construct as it is pointed out by the same authors.

4 PRE-FILTERING BASED ON VISUAL ILLUSION

For solving the dynamic range problem by using the standard displaying system, we next propose a method for generating display images based on visual illusions in intensity.

In our method, we do not modify the dynamic range of the input image S_i. In stead of modifying the dynamic range of S_i, we simply cut out the out of range intensity in the deconvolution image S_i' as follows:

$$\begin{aligned} S_i''(x,y) &= C[S_i'(x,y)] \\ &= C[P(x,y)^{-1} * S_i(x,y)] \end{aligned} \tag{7}$$

where, $C[I]$ is a cut out function which takes the following values according to the intensity I:

$$C[I] = \begin{cases} 0 & (I < 0) \\ 255 & (I > 255) \\ I & (\text{otherwise}) \end{cases} \tag{8}$$

However, S_i'' is no longer identical with S_i', and thus the observed image S_o of S_i'' is not identical with the original image S_i as follows:

$$\begin{aligned} S_o(x,y) &= P(x,y) * S_i''(x,y) \\ &= P(x,y) * C[P(x,y)^{-1} S_i(x,y)] \\ &\neq S_i(x,y) \end{aligned} \tag{9}$$

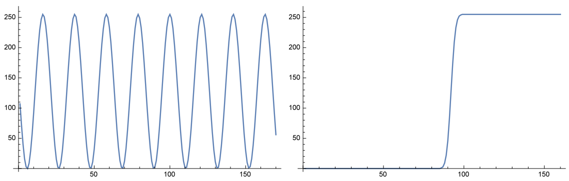

(a) sinusoidal signal (b) step signal

Figure 3: The original image signals used in our experiments. (a) is a sinusoidal signal and (b) is a step signal.

Thus, what we need to do is to find a display image $S_i''(x,y)$, which minimizes the following observation error E:

$$E = \sum_x \sum_y ||S_i(x,y) - P(x,y) * S_i''(x,y)||^2 \tag{10}$$

As we have seen in section 2, the human visual system can perceive higher dynamic range images than those shown by the display system. Thus, by using this property, we may be able to derive better display images for human observers. For counting the lateral inhibition $L(x,y)$ in human vision system, we consider the following observation error E' instead of E in Eq.(10):

$$\begin{aligned} E' = \sum_x \sum_y ||&L(x,y) * S_i(x,y) \\ &- L(x,y) * P(x,y) * S_i''(x,y)||^2 \end{aligned} \tag{11}$$

However, $S_i''(x,y)$ does not have enough freedom to minimize E' effectively. Thus, we consider a high resolution image $S_i''(x',y')$ as the display image, and derive the high resolution display image $S_i''(x',y')$ which minimizes the following observation error E'':

$$\begin{aligned} E'' = \sum_x \sum_y ||&L(x,y) * S_i(x,y) \\ &- D[L(x',y') * P(x',y') * S_i''(x',y')]||^2 \end{aligned} \tag{12}$$

where, $D[\cdot]$ denotes the down sampling from high resolution to the original image resolution, and $L(x',y')$ and $P(x',y')$ represent lateral inhibition and PSF in high resolution. Assuming the lateral inhibition and the PSF of the observer are known, the optimum display image $S_i''(x',y')$ can be derived from the objective image $S_i(x,y)$ by minimizing E''.

5 EXPERIMENTS

We next show the efficiency of the proposed method by using synthetic image signals and real images.

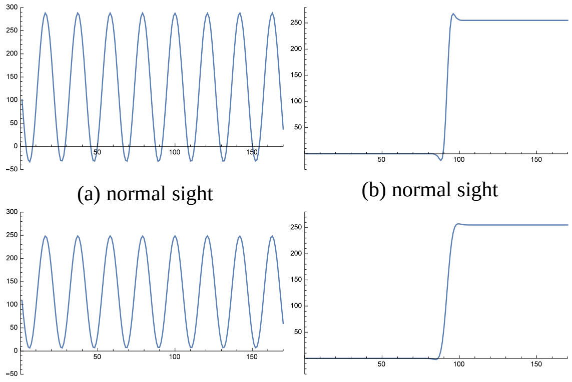

(a) normal sight (b) normal sight

(c) weak sighted (d) weak sighted

Figure 4: The images observed by a normal sight observer and a weak-sighted observer. (a) and (b) show the observation of the normal sight observer, and (c) and (d) show the observation of the weak-sighted observer respectively.

5.1 Synthetic Image Experiments

We first show results from synthetic image signals. Fig. 3 (a) and (b) show two different original image signals. (a) is a sinusoidal signal and (b) is a step signal. In this experiment, we assume that the lateral inhibition of human observer is modeled by Eq.(3), where the standard deviation of the Gaussian function is 1.0 pixel and $\alpha = 3.0$. The PSF of the weak-sighted observer is a Gaussian function with the standard deviation of 2.5 pixels. Then, Fig. 4 (a) and (b) show the observation of a normal sight observer, and (c) and (d) show the observation of the weak-sighted observer. As shown in (c) and (d), the observations of the weak-sighted observer are blurred. Also, the observed intensity range of the weak-sighted observer is smaller than that of the normal sight observer.

We derived display images for weak-sighted observer by using four different methods, that is (1) existing method, (2) lateral inhibition method, (3) high resolution method, and (4) lateral inhibition with high resolution method. The existing method derives display images based on Eq.(7). The lateral inhibition method derives display images which minimize Eq.(10). The high resolution method derives display images based on Eq.(11). The lateral inhibition with high resolution method derives display images which minimize Eq.(12). The number of image pixels in the high resolution display is twice of that in the normal resolution display in this experiment. i

The left column of Fig. 5 shows display images generated by using these four methods, and the right column of Fig. 5 shows images observed by a weak-sighted observer. The red lines show observed images and the blue lines show their ground truth. The RMS errors of observed images are also shown in the right column. Fig. 6 shows the results from the step signal.

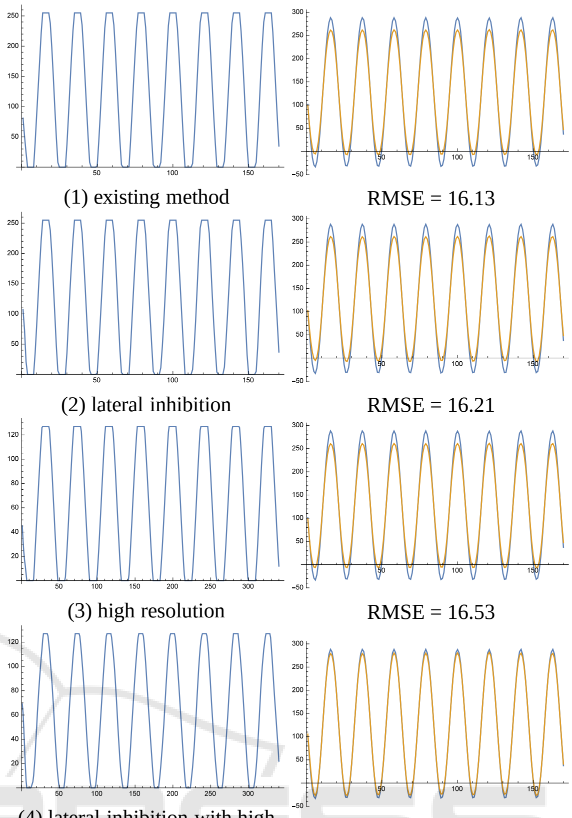

(1) existing method RMSE = 16.13

(2) lateral inhibition RMSE = 16.21

(3) high resolution RMSE = 16.53

(4) lateral inhibition with high resolution RMSE = 4.46

Figure 5: The display images and observed images. The left column shows display images generated from (1) existing method, (2) lateral inhibition method, (3) high resolution method, and (4) lateral inhibition with high resolution method. The red lines in the right column show these images observed by a weak-sighted observer and the blue lines show the ground truth of observed images.

As shown in these images, the simple lateral inhibition and the simple high resolution method do not provide us better results. However, the proposed lateral inhibition with high resolution method provides us much better results than the existing methods and other methods. Note, the proposed method enables us to observe negative intensities and over range intensities accurately as shown in Fig. 5 (d) and Fig. 6 (d). These results show the efficiency of the combination of lateral inhibition and high resolution in the proposed method.

5.2 Real Image Experiments

We next show results from real image experiments. Fig. 7 (a) and (b) show original images used in our experiments. The lateral inhibition and the PSF of a weak-sighted observer is the same as those used in

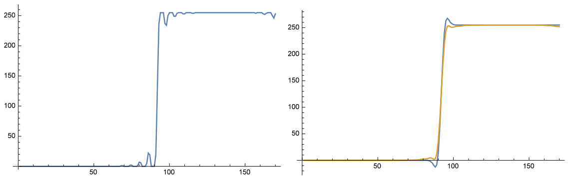

(1) existing method RMSE = 4.33

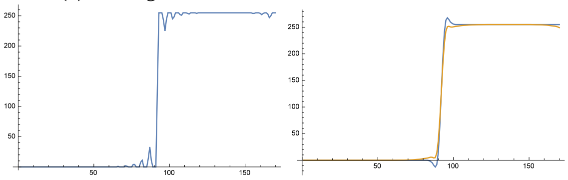

(2) lateral inhibition RMSE = 4.65

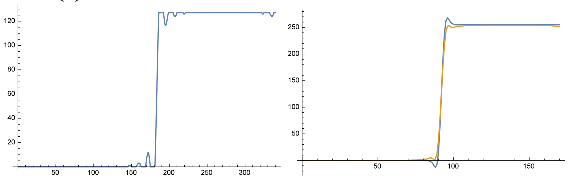

(3) high resolution RMSE = 4.46

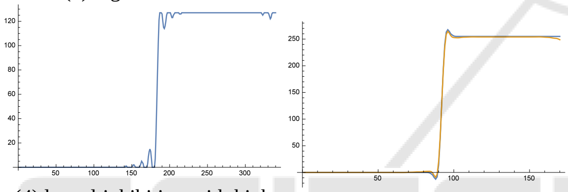

(4) lateral inhibition with high resolution RMSE = 1.73

Figure 6: The display images and observed images. The left column shows display images generated from (1) existing method, (2) lateral inhibition method, (3) high resolution method, and (4) lateral inhibition with high resolution method. The red lines in the right column show these images observed by a weak-sighted observer and the blue lines show the ground truth of observed images.

(a) (b)

Figure 7: The images used in our real image experiments.

the synthetic image experiments. Fig. 4 (a) and (b) show the observation of a normal sight observer, and (c) and (d) show the observation of the weak-sighted observer.

We derived display images for weak-sighted observer by using the existing method and the proposed method which combines the lateral inhibition with

(a) display image (b) observed image

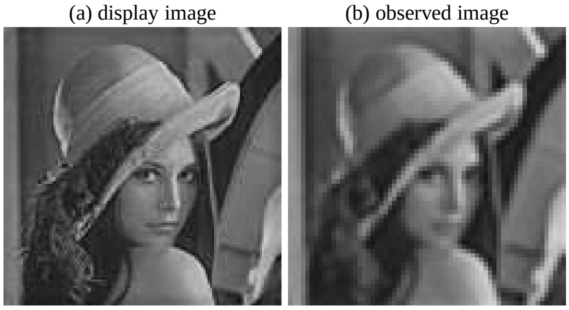

(c) display image (d) observed image

Figure 8: (a) and (b) show the display image and the observed image of a weak sighted observer in the existing method. (c) and (d) show those in the proposed method.

high resolution displaying. Fig. 8(a) shows the display image derived from the existing method, and (b) shows the image observed by a weak-sighted observer. Fig. 8(c) shows the display image derived from the proposed method, and (d) shows the image observed by a weak-sighted observer. Fig. 9 shows the results from another image. Note, the resolution of the observed images in the proposed method is same as that in the existing method. As shown in Fig. 8 (b) and (d) and Fig. 9 (b) and (d) , the proposed method provides us better observation for weak-sighted observer. This is because the proposed method uses the lateral inhibition in human observers efficiently.

Fig. 10 shows the comparison of the frequency characteristics of observed images in the existing method and the proposed method, i.e. lateral inhibition with high resolution. Fig. 10 (a) is the frequency characteristic of the ground truth observation of Fig. 7 (a). Fig. 10 (b) is that of the existing method, and (c) is that of the proposed method. As shown in these images, both the existing method and the proposed method lose high frequency components. However, the proposed method can preserve more high frequency components than the existing method. Since the high frequency components correspond to the sharpness of images, these results confirm that the weak-sighted people can observe better images.

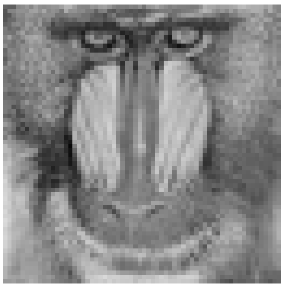

(a) display image (b) observed image

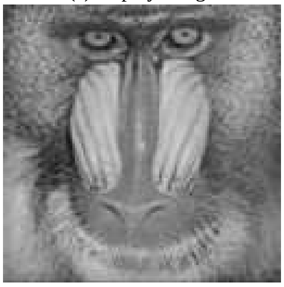

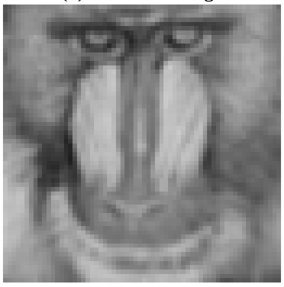

(c) display image (d) observed image

Figure 9: (a) and (b) show the display image and the observed image of a weak sighted observer in the existing method. (c) and (d) show those in the proposed method.

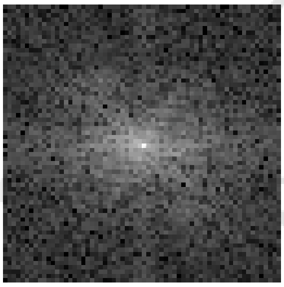

(a) ground truth

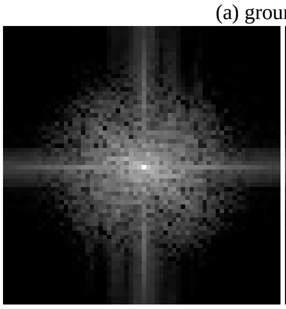

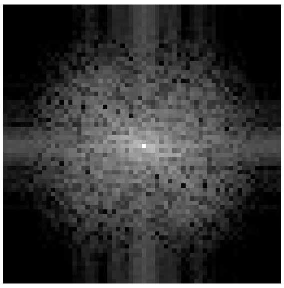

(b) existing method (c) proposed method

Figure 10: The frequency characteristics of observed images. (a) is the ground truth, (b) is the observation in the existing method, and (c) is the observation in the proposed method.

6 CONCLUSION

In this paper, we proposed a method for displaying visual information for weak-sighted people to see clear images on the display. For this objective, we used the lateral inhibition which causes visual illusions in human visual systems. The lateral inhibition enhances input signals and thus the human visual systems can observe wider dynamic range than that in the display device. By using this property, we generated the optimum display images for weak-sighted observed to see original clear images without wearing glasses and contact lenses. We showed that the lateral inhibition works efficiently by combining it with high resolution displaying. The efficiency of the proposed method is tested by using synthetic images and real images.

REFERENCES

Alonso, M. and Barreto, A. (2003). Pre-compensation for high-order aberrations of the human eye using on-screen image deconvolution. In *Proc. Annual International Conference of the IEEE EMBS*, pages 556–559.

Chevreul, M. (1890). *The Principles of Harmony and Contrast of Colors*. George Bell and Sons.

Huang, F., Lanman, D., Barsky, B., and Raskar, R. (2012). Correcting for optical aberrations using multilayer displays. In *Proc. ACM SIGGRAPH Asia*.

Huang, F., Wetzstein, G., Barsky, B., and Raskar, R. (2014). Eyeglass-free display: Towards correcting visual aberrations with computational light field display. In *Proc. ACM SIGGRAPH*.

Marr, D. and Hildreth, E. (1980). Theory of edge detection. *Proceedings of Royal Society of London*, B(27):187–217.

Ratliff, F. (1965). *Mach Bands: Quantitative Studies on Neural Networks in the Retina*. Holden Day.

Wetzstein, G., Lanman, D., Hirsch, M., and Raskar, R. (2012). Tensor displays: Compressive light field synthesis using multilayer displays with directional backlighting. In *Proc. ACM SIGGRAPH*.